Molecular Neurobiology (2019) 56:5971–5986
https://doi.org/10.1007/s12035-019-1481-x

Fingolimod Suppresses the Proinflammatory Status of Interferon-γ-Activated Cultured Rat Astrocytes

Saša Trkov Bobnar[1,2] · Matjaž Stenovec[1,2] · Katarina Miš[3] · Sergej Pirkmajer[3] · Robert Zorec[1,2]

Received: 25 October 2018 / Accepted: 10 January 2019 / Published online: 30 January 2019

Abstract

Astroglia, the primary homeostatic cells of the central nervous system, play an important role in neuroinflammation. They act as facultative immunocompetent antigen-presenting cells (APCs), expressing major histocompatibility complex (MHC) class II antigens upon activation with interferon (IFN)-γ and possibly other proinflammatory cytokines that are upregulated in disease states, including multiple sclerosis (MS). We characterized the anti-inflammatory effects of fingolimod (FTY720), an established drug for MS, and its phosphorylated metabolite (FTY720-P) in IFN-γ-activated cultured rat astrocytes. The expression of MHC class II compartments, β_2 adrenergic receptor (ADR-β_2), and nuclear factor kappa-light-chain enhancer of activated B cells subunit p65 (NF-κB p65) was quantified in immunofluorescence images acquired by laser scanning confocal microscopy. In addition, MHC class II-enriched endocytotic vesicles were labeled by fluorescent dextran and their mobility analyzed in astrocytes subjected to different treatments. FTY720 and FTY720-P treatment significantly reduced the number of IFN-γ-induced MHC class II compartments and substantially increased ADR-β_2 expression, which is otherwise small or absent in astrocytes in MS. These effects could be partially attributed to the observed decrease in NF-κB p65 expression, because the NF-κB signaling cascade is activated in inflammatory processes. We also found attenuated trafficking and secretion from dextran-labeled endo-/lysosomes that may hinder efficient delivery of MHC class II molecules to the plasma membrane. Our data suggest that FTY720 and FTY720-P at submicromolar concentrations mediate anti-inflammatory effects on astrocytes by suppressing their action as APCs, which may further downregulate the inflammatory process in the brain, constituting the therapeutic effect of fingolimod in MS.

Keywords Astrocytes · Antigen-presenting cells (APCs) · Major histocompatibility complex (MHC) class II molecules · Interferon-γ · Fingolimod

Introduction

Astrocytes are the primary homeostatic cells of the central nervous system (CNS), where they play a major role in ion, water, and neurotransmitter homeostasis [94], regulate energy metabolism [8], synaptic transmission [2], blood–brain barrier (BBB) integrity [1], brain microcirculation [36], and have an important role in neuroinflammation [26]. Moreover, dysfunctional astrocytes emerge as key players in the pathology of several neurologic diseases [21], such as multiple sclerosis (MS) [20], amyotrophic lateral sclerosis [64], Parkinson's disease [35], Alzheimer's disease [50], and epilepsy [82].

MS is thought to be an autoimmune disease whereby activated, myelin-reactive T cells migrate into the CNS through the compromised BBB [56]. Reactivation of the T cells by CNS-resident antigen-presenting cells (APCs), which present myelin antigens, triggers the recruitment of innate immune cells, which have important roles in mediating demyelination and axonal damage [32]. Myelin-reactive $CD4^+$ T cells release proinflammatory cytokines, such as interferon (IFN)-γ, interleukin (IL)-17, and granulocyte/macrophage colony-stimulating factor (GM-CSF) [12]. These factors, in particular IFN-γ, can induce glial cells to express major histocompatibility complex (MHC) class II molecules, which are required to present myelin antigens to the T cells in order to mount an autoimmune response [74].

✉ Robert Zorec
robert.zorec@mf.uni-lj.si

[1] Laboratory of Neuroendocrinology-Molecular Cell Physiology, Institute of Pathophysiology, Faculty of Medicine, University of Ljubljana, Zaloška 4, 1000 Ljubljana, Slovenia

[2] Celica Biomedical, Tehnološki park 24, 1000 Ljubljana, Slovenia

[3] Laboratory for Molecular Neurobiology, Institute of Pathophysiology, Faculty of Medicine, University of Ljubljana, Zaloška 4, 1000 Ljubljana, Slovenia

Both microglia and astrocytes can function as APCs in the brain. In contrast to microglia, which constitutively express MHC class II antigens, astrocytes are facultative immunocompetent APCs that have the ability to express MHC class II antigens, adhesion molecules (ICAM-1, VCAM-1), and costimulatory signals (B7-1 and B7-2) [28, 60, 80, 99, 100] only upon activation with IFN-γ and possibly other proinflammatory cytokines, such as IL-17 and GM-CSF, that appear to be upregulated in the CNS in the condition of MS [12]. Several studies have reported the presence of MHC class II molecules on astrocytes in MS [48, 67, 83, 100]; however, a number of studies failed to detect them [5, 11, 37]. In contrast to microglia, endogenous suppressor molecules, including norepinephrine, regulate MHC class II expression in astrocytes. The effects of norepinephrine are mediated through activation of β_2 adrenergic receptors (ADR-β_2), which are prominently expressed in reactive astrocytes [22]. In MS brain tissue samples, ADR-β_2 are absent on astrocytes, not only in chronic active and inactive plaques but also in normal-appearing white matter, whereas they are normally present on neurons [22, 98]. Because astrocytic ADR-β_2 are involved in suppressing inducibility of MHC class II molecules, it has been suggested that the loss of these receptors likely facilitates the induction of astrocytes to function as facultative immunocompetent APCs [23]. A role of astrocytes as facultative APCs in MS is supported by the findings that scattered astrocytes in active MS lesions express MHC class II [100] and B-7 costimulatory molecules [99]. Moreover, it has been shown that primary mice astrocytes have potential for processing and presenting CNS autoantigens to proinflammatory T cells [74].

Fingolimod (FTY720; GILENYA, Novartis Pharma AG, Basel, Switzerland) was the first oral disease-modifying therapy to be approved for relapsing forms of MS [17, 42, 47]. Although the phosphorylated form, FTY720-phosphate (FTY720-P), is considered to be responsible for the beneficial effects in MS treatment by acting on *sphingosine-1-phosphate* (S1P) receptors on lymphocytes, causing lymphopenia, accumulating evidence is revealing that FTY720 exerts neuroprotective effects by acting directly on the brain cells, in particular on astrocytes [59]. Due to its lipophilic nature, FTY720 readily crosses the BBB and accumulates in the CNS white matter [27]. CNS concentrations of the parent drug and its phosphorylated metabolite reach comparable levels [27], suggesting that an equilibrium is established due to endogenous sphingosine kinase (SphK) 2-mediated phosphorylation [3]. S1P receptors are widely expressed on the CNS cells, with region-specific distributions [18]; however, other mechanisms that act independently of S1P receptors may also be part of the FTY720 activity, such as suppression of eicosanoid production due to inhibition of cytosolic phospholipase A2 [63], attenuated vesicle traffic and exocytotic secretion [84], and alteration of calcium homeostasis [77] in astrocytes.

In this study, we asked whether FTY720 and FTY720-P affect the function of astroglial facultative APCs in the context of brain inflammatory conditions in MS. We investigated how FTY720 and FTY720-P affect the expression of MHC class II molecules, ADR-β_2, and subcellular localization of nuclear factor kappa-light-chain-enhancer subunit p65 (NF-κB p65), a molecule related to the inflammatory status of cells, in IFN-γ-activated astrocytes. At therapeutically relevant nanomolar concentrations [57], both molecules exerted anti-inflammatory effects, indicating an additional clinically relevant therapeutic action of fingolimod as an immunomodulatory drug acting directly on astroglia.

Materials and Methods

Cell Culture

Primary astrocyte cultures were prepared from neocortices of 3-day-old female Wistar rats (obtained from Medical Experimental Centre at the Institute of Pathology, University of Ljubljana, Slovenia) as described [72]. Care of the experimental animals was in accordance with European and Slovenian legislation (Official Gazette of the RS 38/13; UVHVVR, no. U34401-47/2014/7). Cells were grown in high-glucose (25 mM) Dulbecco's modified Eagle's medium containing 10% fetal bovine serum (Biochrom AG, Berlin, Germany), 1 mM sodium pyruvate, 2 mM L-glutamine, and 5 U/ml penicillin/5 μg/ml streptomycin in an atmosphere of 5% CO_2/95% air. To purify isolated cells, subconfluent cultures were shaken three times at 225 rpm overnight with subsequent medium change. Before the experiments, cells were trypsinized, subcultured onto poly-L-lysine (PLL)-coated coverslips or multiwell plates, and maintained at 37 °C in an atmosphere of 5% CO_2/95% air. Unless stated otherwise, all chemicals were purchased from Sigma-Aldrich (Germany) and were of the highest purity grade available.

Cell Treatments

The next day after seeding, the growth medium was changed (in controls) or cells were treated with growth medium supplemented with 600 U/mL IFN-γ (Hycult Biotech, The Netherlands), 600 U/mL IFN-γ and 0.1 μM FTY720 (Enzo Life Sciences, USA), 600 U/mL IFN-γ and 0.1 μM FTY720-P (Echelon Biosciences, USA), or the growth medium containing 0.1 μM FTY720 or 0.1 μM FTY720-P alone. To examine the dose dependency of FTY720 treatment, IFN-γ-activated cells were also treated with 0.01 and 0.5 μM FTY720. All treatments lasted for 48 h, during which cells were maintained at 37 °C in an atmosphere of 5% CO_2/95% air.

Cell Counts and Diameter

Cells were seeded in P12 or P24 plates and exposed to a 48-h treatment regime (as described above) in duplicate/triplicate for each condition. Subsequently, cells were trypsinized and analyzed by a Scepter 2.0 Handheld Automated Cell Counter (Merck, Germany), which displays the cell size distribution profile. Gating by the minimal and maximal cell diameter was set uniformly to exclude aberrantly large (cell clumps) or small particles (debris). Cell counts were expressed relatively (as a percentage) as the average cell count of treated cells (in triplicates) versus the average cell count of non-treated controls for each experiment. The average relative cell count and cell diameter were pooled from four to six individual experiments.

Immunocytochemistry

Cells were seeded on PLL-treated coverslips and exposed to the cell treatment regime for 48 h as described above. Upon cell treatment, astrocyte-loaded coverslips were washed with phosphate-buffered saline (PBS, 3 min) and fixed in paraformaldehyde (4% in PBS) for 15 min, permeabilized with 0.1% Triton X-100 for 10 min, and then washed 3× with PBS. The non-specific background staining was reduced by incubating cells in a blocking buffer with 10% (*v*/*v*) goat serum in 3% bovine serum albumin (BSA) in PBS for 1 h at 37 °C. Cells were then washed 1× with PBS and incubated with the following primary antibodies diluted in 3% BSA in PBS overnight at 4 °C: mouse anti-glial fibrillary acidic protein (GFAP; 1:100, G3893, Sigma-Aldrich, Germany), anti-ionized calcium-binding adapter molecule 1 (Iba-1; 1:100, Ab15691, Abcam, UK), mouse anti-MHC II (1:100; ab23990, Abcam, UK), rabbit anti-ADR-β_2 (1:100; orb10056, Biorbyt, UK), and mouse anti-NF-κB (1:100; sc-8008, Santa Cruz Biotechnology, USA). Incubation with the primary antibody was followed by 4× 3-min washes in PBS and the addition of the respective fluorescent secondary antibody (goat anti-rabbit/anti-mouse conjugated to Alexa Fluor 488/546, diluted 1:600 in 3% BSA in PBS; Thermo Fisher Scientific, CA, USA) at 37 °C for 45 min. Incubation with the secondary antibody was followed by 4× 3-min washes in PBS, and afterward, the coverslips were mounted onto glass slides using Slow Fade Gold Antifade Mountant with DAPI (Thermo Fisher Scientific, USA).

Cells were examined with a laser scanning fluorescence confocal microscope (LSM 780; Zeiss, Germany) equipped with a plan-apochromatic oil-immersion objective ×63/NA 1.4. Alexa Fluor 488/546 was excited by a 488-nm argon laser line or 561-nm diode-pumped solid-state laser, and the fluorescence emission was bandpass filtered at 500–550 or 565–615 nm, respectively. DAPI was excited by a 405-nm diode-pumped solid-state laser, and emission was bandpass filtered at 440–480 nm. We recorded 15–20 images per coverslip.

Quantification of the Immunofluorescence Staining

Quantitative analysis of the immunofluorescence images was performed by ImageJ software (NIH, Bethesda, MD, USA) using the particle count function (for MHC II) or pixel area measurements (for ADR-β_2, NF-κB p65) by pre-setting a constant threshold for each set of treatments (typically at 20–30% of the maximal fluorescence). The particle count or pixel area above the threshold was normalized to the cell number in individual images. The latter was determined manually by counting DAPI-stained nuclei. Protein expression was quantified in the *x*,*y* images depicting individual cell planes (of 2 μm thickness). The average values from 15 to 20 images acquired in each coverslip were calculated. The number of coverslips examined ranged from 4 to 15, depending on the particular treatment.

To quantify the fluorescence of the NF-κB p65 total and nuclear signal, first the co-localization of red (immunofluorescent NF-κB p65) and blue (DAPI) signals was analyzed with ColocAna software (Celica, Ljubljana, Slovenia). The program counted all red, blue, and co-localized (red and blue) pixels in individual images. The threshold for the pixel count was set to 20% of the maximal fluorescence to reduce noise and fluorescence overlap originating from closely positioned labeled structures. Total and nuclear NF-κB p65 protein expression was determined by the number of red and co-localized pixels, respectively, normalized to the number of nuclei in the images and expressed relatively to the control (untreated) condition.

Extraction of mRNA and Quantitative Real-Time Polymerase Chain Reaction

Rat astrocytes were cultured in six-well plates and exposed to a 48-h treatment regime (as described above). Total RNA was extracted from cultured astrocytes with the RNeasy Mini Plus Kit (Qiagen, Germany). cDNA was synthesized from total RNA using the High-Capacity cDNA Reverse Transcription Kit (Applied Biosystems, Thermo Fisher Scientific, Lithuania). Quantitative polymerase chain reaction (qPCR) was performed on an ABI PRISM SDS 7500 (Applied Biosystems, Thermo Fisher Scientific, USA) in a 96-well format using TaqMan Universal PCR Master Mix (Applied Biosystems, Thermo Fisher Scientific, USA) and gene expression assays for ADR-β_2 (Adrb2, Rn00560650_s1) and 18S rRNA (TaqMan Endogenous Control). Standard quality controls were performed in line with the MIQE (minimum information necessary for evaluating qPCR experiments) guidelines [10]. The expression level of ADR-β_2 mRNA was calculated as the gene expression ratio (ADR-β_2 mRNA/18S

rRNA) according to the equation: $E_{18S\ rRNA}^{Ct,18S\ rRNA}/E_{ADR\beta2}^{Ct,\ ADR\beta2}$, where E is the PCR efficiency and Ct is the threshold cycle for the reference (18S rRNA) or the target (*Adrb2*) gene [69, 85]. PCR efficiency was estimated using the LinRegPCR program gene [69, 85].

Vesicle Mobility

Cells were seeded on PLL-treated coverslips and treated with 600 U/mL IFN-γ or co-treated with 600 U/mL IFN-γ and 0.1 mM FTY720 or 0.1 mM FTY720-P for 48 h. During the cell treatment, 0.1 mg/mL dextran conjugated to Alexa Fluor 546 (10,000 Da; Thermo Fisher Scientific, USA) was added to the culture medium to allow loading of fluorescent dextran into vesicles by the endocytic pathway at 37 °C overnight. The next day, astrocyte-loaded coverslips were washed 2× with extracellular solution containing 130 mM NaCl, 5 mM KCl, 2 mM $CaCl_2$, 1 mM $MgCl_2$, 10 mM D-glucose, and 10 mM HEPES (pH 7.2), mounted onto the recording chamber, and transferred to a confocal microscope (LSM 780; Zeiss, Germany) equipped with a plan-apochromatic oil immersion objective ×63/NA 1.4. Dextran Alexa Fluor 546 fluorescence was excited by a 561-nm diode-pumped solid-state laser, and the fluorescence emission was bandpass filtered at 565–615 nm. Time-lapse images were acquired every 485 ms for 1 min before and 3 min after stimulation with 100 μM adenosine 5′-triphosphate (ATP). The mobility of dextran-laden vesicles was analyzed by ParticleTR software (Celica, Ljubljana, Slovenia) in exported tiff files as described previously [65]. Briefly, a 3D Gaussian curve was fitted onto a selected vesicle in each image to obtain the x, y coordinates (peak of the curve), which were then connected to obtain the pathways that vesicles traveled within the total recording time. Typically, 50 randomly selected vesicles were tracked per cell, and for each vesicle, the track length (TL, the pathway that an individual vesicle traveled), maximal displacement (MD, the farthest translocation of a vesicle), and the directionality index (DI = MD/TL) were determined. The mobility parameters were estimated for 15-s epochs. The analysis of the vesicle mobility was performed in cells activated with IFN-γ, and IFN-γ-activated cells co-treated with 0.1 mM FTY720 or 0.1 mM FTY720-P for 48 h. The mean (± SE) vesicle TL, MD, and DI values were determined in seven to eight cells per treatment.

Vesicle Cargo Release

The ATP-evoked cargo release from dextran-labeled vesicles was analyzed from the time-lapse recordings obtained as described above. The possible modulation of FTY720 or FTY720-P treatment on stimulated vesicle secretion from IFN-γ-activated astrocytes was determined by two different approaches: by counting fluorescent vesicles at different time points upon stimulation with 100 μM ATP and by observing individual cargo discharge events as sudden decreases in the vesicle fluorescence. The numbers of dextran-laden vesicles were obtained by ImageJ software (NIH, Bethesda, MD, USA) using the Analyse Particle function. To identify individual vesicles, the intensity threshold was set to 20% of the maximum fluorescence and the minimum particle size to three adjacent pixels (3 × 0.132 × 0.132 μm), and thus the minimum surface area covered by a particle was 0.052 μm^2. The vesicles were counted on three/five consecutive confocal images taken at time 0 and 1, 2 and 3 min after stimulation with ATP. The relative decrease in vesicle number was obtained as the difference in the average vesicle numbers at different time points after stimulation with respect to the initial vesicle number at time 0. The vesicle numbers at different time points were counted in four to five cells. Alternatively, individual full-collapse exocytotic events resulting in discharge of fluorescent dextran were identified as a sudden decrease in the vesicle fluorescence [75] and counted manually. At the location of individual secreting vesicles, the changes in time-resolved fluorescence were obtained by the LSM 780 software (Zeiss) using a circular region of interest ($r = 0.528$ μm, $S = 0.876\ \mu m^2$).

Statistical Analysis

The relative cell counts, diameter, compartment number, surface area, vesicle mobility parameters, and vesicle counts were expressed as the mean ± SE. Statistical significance was determined with one-way analysis of variance (ANOVA) and the differences in the vesicle mobility parameters (TL, MD, and DI) and secretion were analyzed by the two-tailed Student's t test using SigmaPlot 11.0 (Systat Software Inc., USA).

Results

IFN-γ Activation and Treatment with FTY720 or FYT720-P Minutely Affects the Cell Count but Not the Diameter of Cultured Rat Astrocytes

To confirm that astrocytes were isolated in a highly enriched culture devoid of microglia, cells were immunofluorescently labeled with antibody against astrocytic marker GFAP (Fig. 1a) and microglial marker Iba-1 (Fig. 1b). This immunostaining demonstrated that the cultures were ~ 100% positive for GFAP marker, as reported previously [78], whereas no Iba-1-positive cell was observed, confirming the purity of the isolated astrocytic culture.

Next, we assessed the effects of different treatments on the proliferation capacity of cultured astrocytes. We measured the total cell counts at the end of each treatment regime. The

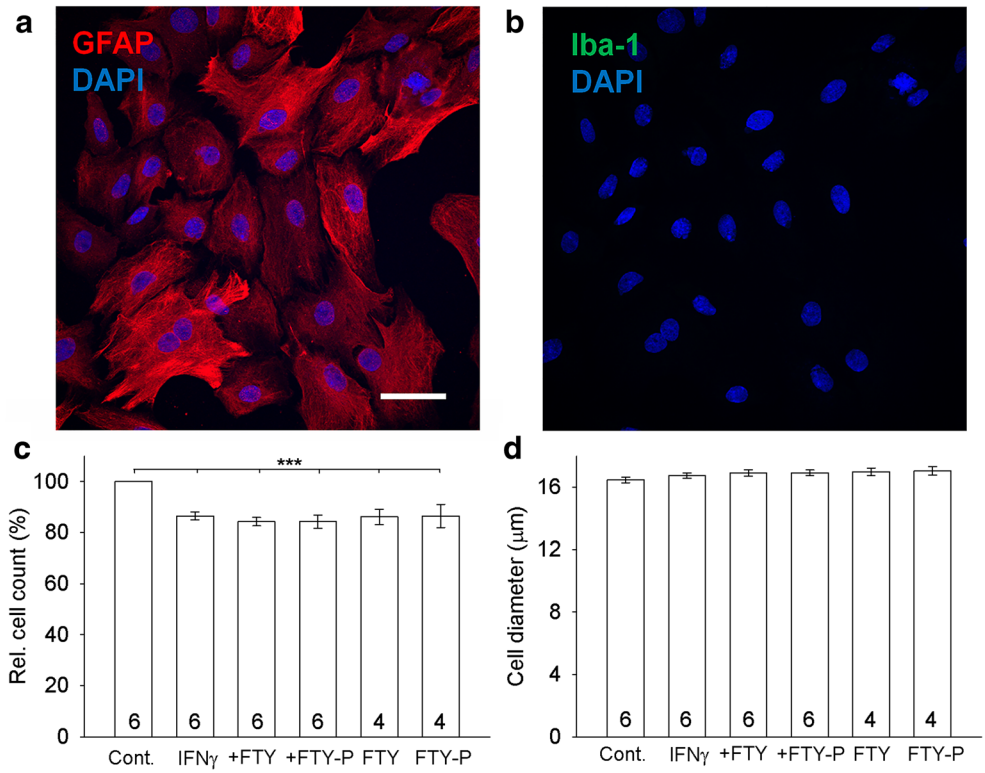

Fig. 1 **a, b** Cell properties in non-treated and IFN-γ-activated astrocytes, co-treated with FTY720 or FTY720-P. Cultured rat astrocytes were immunofluorescently labeled with astrocyte marker GFAP (red) and microglial marker Iba-1 (green); nuclei were stained with DAPI (blue). Practically all the cells (~ 100%, $N = 4$ from three cell preparations) stained positively with anti-GFAP (**a**), but not with anti-Iba-1 (**b**), demonstrating preparation of a pure astrocyte culture devoid of microglia. Scale bar, 20 μm. **c**, **d** Plots displaying relative cell counts (**c**) and the respective cell diameters, determined by Coulter counter (**d**) of IFN-γ-activated astrocytes (IFN-γ) co-treated with 0.1 μM FTY720 (+FTY) or 0.1 μM FTY720-P (+FTY-P) and cells solely treated with 0.1 μM FTY720 (FTY) or 0.1 μM FTY720-P (FTY-P), versus non-treated controls (Cont). **c** All treatments caused a relative decrease in cell counts when compared with the control cells (***$P \leq 0.001$); however, there was no statistically significant difference between different cell treatments. **d** The average cell diameter measured in controls and treated cells demonstrates that the cell treatment did not evoke major changes in cell volume. The numbers at the base of the bars indicate the number of experiments (in triplicate) for each treatment. ***$P \leq 0.001$ versus control

relative cell numbers of treated cells with respect to control conditions (100%) were 86.5 ± 1.6, 84.3 ± 1.7, 84.3 ± 2.5, 86.1 ± 3.1, and 86.5 ± 4.6% (all $P \leq 0.001$) for IFN-γ, IFN-γ + FTY720, IFN-γ + FTY720-P, FTY720, and FTY720-P-treated cells, respectively (Fig. 1c). All cell treatments caused a minor (12–18%), although significant decrease in cell counts compared with the control; however, there was no statistically significant difference in cell counts between different treatments. These results showed that IFN-γ treatment had a minor effect on the extent of cell counts, whereas the addition of FTY720 or FTY720-P did not further affect the cell count. The sole presence of FTY720 or FTY720-P decreased cell numbers to a similar extent as IFN-γ alone. These data rule out potential toxic effects due to long-term (48-h) cell exposure to 0.1 μM FTY720 or 0.1 μM FTY720-P (applied alone or in combination with 600 U/mL IFN-γ).

None of the treatments significantly affected cell diameter, which was on average 16.5 ± 0.2, 16.8 ± 0.2, 16.9 ± 0.2, 16.9 ± 0.2, 17.0 ± 0.2, and 17.0 ± 0.3 μm for control, IFN-γ, IFN-γ + FTY720, IFN-γ + FTY720-P, FTY720, and FTY720-P-treated cells, respectively (Fig. 1d). It was measured in cell suspensions immediately after cell detachment upon the given treatment. These data indicate that the cell treatments did not induce significant changes in cell volume, which could be one of the parameters correlated with potentially induced changes in cell morphology.

FTY720 Dose Dependently Attenuates the Expression of MHC Class II Compartments in IFN-γ-Activated Astrocytes

We next investigated the effects of FTY720 and FTY720-P on MHC class II expression in astrocytes in view of their role as facultative APCs. MHC class II expression was determined by counting the MHC class II-positive compartments in confocal images (Fig. 2a). As expected, control astrocytes expressed only a negligible number of MHC class II compartments (0.33 ± 0.14 compartments/cell), whereas 48-h cell activation with IFN-γ (600 U/mL) induced strong MHC class II expression that resulted in 20.8 ± 1.4 ($P \leq 0.0001$) compartments per

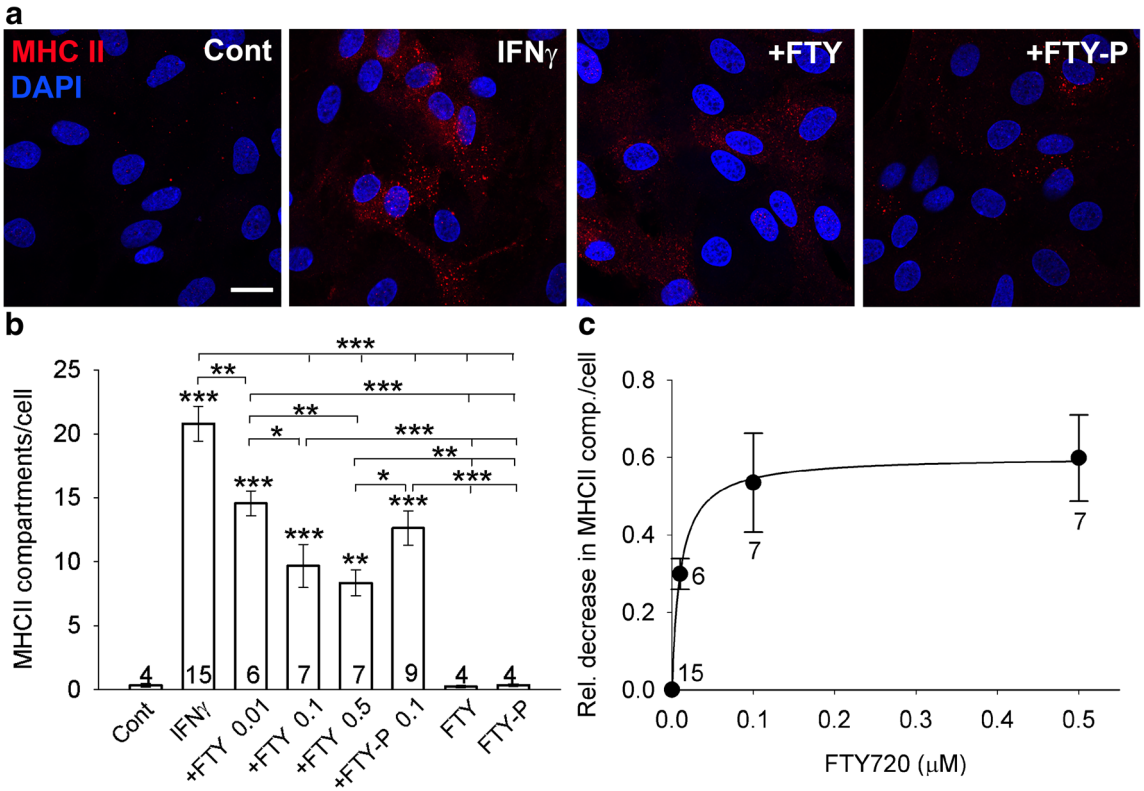

Fig. 2 Cell treatment with FTY720 and FTY720-P reduces the number of MHC class II-positive compartments in IFN-γ-activated astrocytes. **a** Confocal images of control (Cont) astrocytes and IFN-γ-activated astrocytes (IFN-γ) co-treated with 0.1 μM FTY720 (+FTY) or 0.1 μM FTY720-P (+FTY-P) immunolabeled with anti-MHC II antibody (red); cell nuclei were stained with DAPI (blue). Scale bar, 20 μm. **b** The average number of MHC class II compartments per cell image in controls (Cont), astrocytes activated with IFN-γ (IFN-γ), and co-treated either with 0.01 μM FTY720 (+FTY 0.01), 0.1 μM FTY720 (+FTY 0.1), 0.5 μM FTY720 (+FTY 0.5), or 0.1 μM FTY720-P (+FTY-P 0.1) and cells solely treated with 0.1 μM FTY720 (FTY) or 0.1 μM FTY720-P (FTY-P). Control astrocytes and cells treated with FTY720 or FTY720-P alone did not express MHC II-positive compartments, whereas IFN-γ activation strongly induced their expression. Addition of FTY720 (0.01, 0.1, or 0.5 μM) or FTY720-P (0.1 μM) to IFN-γ-activated astrocytes caused a remarkable decrease in the expression of MHC class II-positive compartments. The numbers at the base of the bars indicate the number of coverslips examined for each cell treatment. $*P \le 0.05$, $**P \le 0.01$, $***P \le 0.001$ versus control cells and individual pairs as indicated. **c** Dose-dependent decrease in the relative number of MHC class II compartments expressed as the average number of compartments in astrocytes treated with IFN-γ + FTY720 (0.01, 0.1, or 0.5 μM) versus the number of compartments in cells activated with IFN-γ. The dose-dependent profile of the relative decrease in number of MHC class II compartments (per cell) was obtained by fitting the data points with the ligand binding function with one site saturation: $f = B_{max} \times abs(x) / (K_d + abs(x))$, where $B_{max} = 0.6022$ μM and $K_d = 0.0103$ μM ($R = 0.9995$, $P = 0.0101$). The numbers at the data points (mean ± SE) indicate the number of coverslips examined for each treatment

cell image (Fig. 2b). Importantly, the addition of FTY720 (0.01, 0.1, or 0.5 μM) or FTY720-P (0.1 μM) caused a significant decrease in IFN-γ-induced MHC class II expression (Fig. 2b). The number of MHC class II compartments per cell in IFN-γ-activated astrocytes treated with 0.01, 0.1, and 0.5 μM FTY720 decreased to 14.6 ± 1.0 ($P \le 0.0001$), 9.7 ± 1.7 ($P \le 0.001$), and 8.4 ± 1.0 ($P \le 0.001$) compartments per cell, respectively. Similarly, 0.1 μM FTY720-P caused a decrease in IFN-γ-induced MHC class II expression to 12.6 ± 1.3 ($P \le 0.0001$) compartments per cell. Cell treatment with FTY720 or FTY720-P alone did not induce MHC class II expression (0.24 ± 0.09, 0.35 ± 0.09 compartments/cell, respectively) (Fig. 2b).

FTY720 treatment affected IFN-γ-activated MHC class II expression in a dose-dependent manner (Fig. 2c). The relative decrease in MHC class II expression was 23.0% ± 4.0, 53.5% ± 12.8, and 59.9% ± 11.2% for 0.01, 0.1, or 0.5 μM FTY720 (co-applied with IFN-γ), respectively. The data for the relative dose-dependent decrease in the number of MHC class II compartments per cell were fitted with the ligand binding function with one site saturation: $f = B_{max} \times abs(x) / (K_d + abs(x))$, where $B_{max} = 0.6022$ μM and $K_d = 0.0103$ μM ($R = 0.9995$, $P = 0.0101$). These data revealed that half maximal inhibition of MHC class II molecule expression is achieved by 10.3 nM FTY720 in astrocytes.

FTY720 or FYT720-P Prominently Increases ADR-β_2 Expression in IFN-γ-Activated Astrocytes

Astrocytes in tissue samples from MS brain lack ADR-β_2 [22], therefore we next explored the effects of FTY720 and FTY720-P on ADR-β_2 expression in IFN-γ-activated

astrocytes. In addition, ADR-β_2 signaling is involved in downregulation of MHC class II expression [20]. To explore the ADR-β_2 protein expression, we quantified (Fig. 3b) the ADR-β_2 immunofluorescence in confocal images (Fig. 3a). Whereas IFN-γ activation and cell treatment with FYT720 or FTY720-P alone induced a minor increase, the addition of FYT720 or FTY720-P to IFN-γ-activated cells caused a prominent increase in ADR-β_2 expression (Fig. 3b). In controls, the signal area per cell was 16.5 ± 3.2, and it increased to 28.4 ± 3.0, 58.3 ± 5.8 ($P \leq 0.001$), 57.8 ± 4.6 ($P \leq 0.001$), 24.2 ± 5.5, and 28.4 ± 4.2 ($P \leq 0.05$) in IFN-γ, IFN-γ + FTY720, IFN-γ + FTY720-P, FTY720, and FTY720-P-treated cells, respectively. The relative increase in ADR-β_2 expression with respect to controls was modest in cells treated with IFN-γ, FYT720, or FTY720-P, 1.72-fold (72.37%), 1.46-fold (46.45%), and 1.72-fold (72.50%), respectively, and substantial in cells treated with IFN-γ + FTY720 and IFN-γ + FTY720-P, 3.56-fold (253.57%) and 3.51-fold (250.58%) increase, respectively.

In addition, we determined whether expression of ADR-β_2 mRNA parallels the increases in protein abundance. As estimated by qPCR, ADR-β_2 mRNA levels in astrocytes were unaltered by treatment with FTY720 and FTY720-P, whereas they were decreased ($P \leq 0.05$) by the treatment with IFN-γ (Fig. 3c). These results indicate that increases in ADR-β_2 protein abundance are unlikely due to increased gene transcription.

IFN-γ Increases, Whereas FTY720 and FTY720-P Attenuate the Expression of NF-κB p65

Transcription factor NF-κB is activated in the inflammatory processes, and the first step is the translocation of the p65 subunit to the nucleus [39]. We thus investigated the effect of different treatments on NF-κB p65 expression both in general and specifically by estimating its translocation to the nucleus in confocal images of treated astrocytes (Fig. 4a). The total NF-κB p65 immunofluorescence signal normalized to

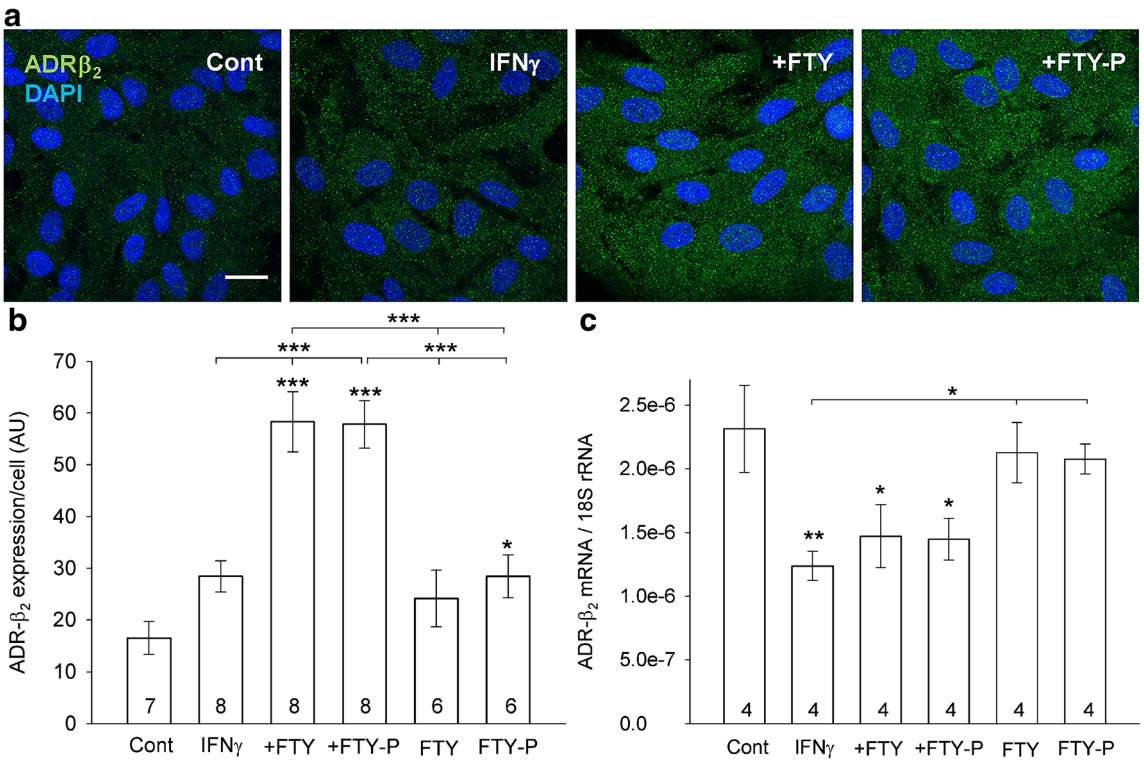

Fig. 3 FTY720 and FTY720-P enhance the expression of ADR-β_2 in IFN-γ-activated astrocytes. **a** Confocal images of non-treated controls (Cont) and IFN-γ-activated astrocytes (IFN-γ) that were treated either with 0.1 μM FTY720 (+FTY) or 0.1 μM FTY720-P (+FTY-P) and immunolabeled with anti-ADR-β_2 antibody (green); nuclei were stained with DAPI (blue). Scale bar, 20 μm. **b** The average (±SE) signal areas of ADR-β_2 immunofluorescence per cell are shown in controls (Cont) and in IFN-γ-activated astrocytes (IFN-γ), co-treated with 0.1 μM FTY720 (+FTY) or 0.1 μM FTY720-P (+FTY-P), and cells solely treated with 0.1 μM FTY720 (FTY) or 0.1 μM FTY720-P (FTY-P). IFN-γ slightly increased ADR-β_2 expression, whereas the addition of FTY720 or FTY720-P caused a prominent increase in ADR-β_2 expression. The numbers at the base of the bars indicate the number of coverslips examined for each treatment. *$P \leq 0.05$, **$P \leq 0.01$, ***$P \leq 0.001$ versus control cells and individual pairs as indicated. **c** The levels (means ± SE) of ADR-β_2 mRNA (qPCR), normalized to 18S rRNA, are shown for astrocytes exposed to different treatments. A decrease in ADR-β_2 mRNA can be observed in IFN-γ-activated astrocytes (IFN-γ). Co-treatment with FTY720 (+FTY) or FTY720-P (+FTY-P) did not cause a statistically significant change in ADR-β_2 mRNA expression versus control (Cont). The numbers at the base of the bars indicate different cell preparations. *$P \leq 0.05$, **$P \leq 0.01$ versus control and individual pairs as indicated

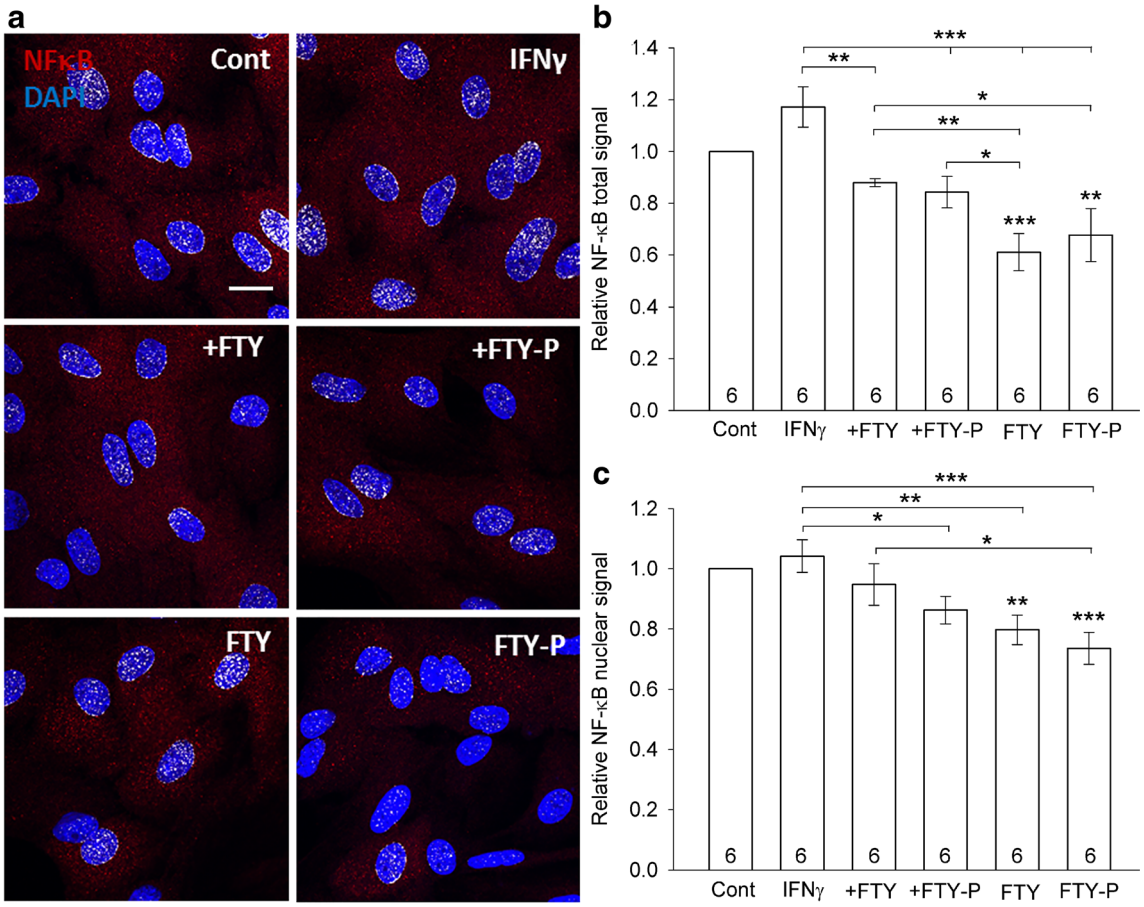

Fig. 4 FTY720 and FTY720-P reduce the total expression and nuclear localization of NF-κB p65. **a** Confocal images displaying immunofluorescent NF-κB p65 (red) in non-treated controls (Cont) and IFN-γ-activated astrocytes (IFN-γ), co-treated either with 0.1 μM FTY720 (+FTY) or 0.1 μM FTY720-P (+FTY-P) or solely treated with 0.1 μM FTY720 (FTY) or 0.1 μM FTY720-P (FTY-P); nuclei stained with DAPI (blue). White pixels show co-localization of NF-κB p65 immunofluorescence with DAPI indicating nuclear localization of NF-κB p65. Scale bar, 20 μm. **b** Quantification of the total NF-κB p65 signal in non-treated controls (Cont) or IFN-γ-activated cells (IFN-γ) treated with 0.1 μM FTY720 (+FTY) and 0.1 μM FTY720-P (+FTY-P) or solely treated with 0.1 μM FTY720 (FTY) or 0.1 μM FTY720-P (FTY-P), expressed with respect to control (non-treated) cells. The treatment with FTY720 or FTY720-P alone and co-application of FTY720 or FTY720-P to IFN-γ-activated cells decreased the total expression of NF-κB p65. **c** Quantification of the co-localized red (NF-κB p65) and blue (DAPI) pixels demonstrating nuclear NF-κB p65, expressed relative to the control (non-treated) cells. Addition of FTY720-P to IFN-γ-activated cells, as well as addition of FTY720 or FTY720-P to non-activated cells, decreased NF-κB p65 translocation to the nuclei. The numbers at the base of the bars indicate the number of coverslips examined for each treated cell. $*P \le 0.05$, $**P \le 0.01$, $***P \le 0.001$ versus control cells and individual pairs as indicated

control was 1.17 ± 0.08, 0.88 ± 0.01, 0.84 ± 0.06, 0.61 ± 0.07 ($P \le 0.001$), and 0.68 ± 0.10 ($P \le 0.01$), in cells treated with IFN-γ, IFN-γ + FTY720, IFN-γ + FTY720-P, FTY720, and FTY720-P, respectively (Fig. 4b). The treatment with FTY720 or FTY720-P alone decreased the expression of NF-κB p65 by 38.9 and 32.3%, respectively. Co-application of FTY720 or FTY720-P to IFN-γ-activated cells decreased its expression by ~25.0% ($P \le 0.05$) and ~28.1% ($P \le 0.001$) with respect to IFN-γ-activated astrocytes, respectively.

Cell activation with IFN-γ did not affect the nuclear translocation of NF-κB p65; the NF-κB p65 nuclear signal area was 1.04 ± 0.05 with respect to control (Fig. 4c). Similarly, the addition of FYT720 or FTY720-P to IFN-γ-activated cells did not cause a significant decrease in the NF-κB p65 nuclear signal area (0.95 ± 0.07-fold and 0.86 ± 0.05-fold, respectfully) with respect to control. The cell treatment with FTY720 and FTY720-P alone significantly decreased the NF-κB p65 nuclear signal (0.79 ± 0.05, $P \le 0.01$ and 0.74 ± 0.05, $P \le 0.001$, respectively). These data indicate that both compounds applied individually downregulate p65 translocation to the nucleus and thus attenuate the activation of the NF-κB signaling pathway.

FTY720 and FYT720-P Decrease the Mobility of Dextran-Labeled Vesicles in IFN-γ-Activated Astrocytes

Vesicle delivery to the plasma membrane is necessary for the exocytotic release of signaling molecules from the vesicle lumen as well as for the efficient translocation of membrane-

bound molecules to the plasmalemma [33, 93]. It has already been reported that IFN-γ treatment enhances the mobility of dextran-labeled vesicles [89]; therefore, we aimed to examine the effects of FTY720 or FYT720-P on the mobility of vesicles in IFN-γ-activated astrocytes. We monitored the mobility of dextran-labeled vesicles that have been reported to highly co-localize with MHC class II compartments and LAMP1-positive compartments in IFN-γ-treated mouse astrocytes [89]. By analyzing time-lapse recordings of dextran-labeled vesicles, we obtained the paths traveled by individual vesicles (~ 50 per cell) in IFN-γ-activated astrocytes treated with FTY720 or FTY720-P (Fig. 5a). Subsequently, TL, MD, and DI (=MD/TL) were calculated. The results showed that the addition of FTY720 and FTY720-P decreased vesicle TL, MD, and DI in IFN-γ-activated astrocytes. The average vesicle TL in IFN-γ-activated astrocytes was 3.34 ± 0.16 μm, and the addition of FTY720 or FYT720-P to activated cells caused a statistically significant decrease in TL to 2.88 ± 0.13 μm (13.7%, $P \leq 0.05$) and 2.87 ± 0.09 μm (14.1%, $P \leq 0.05$), respectively (Fig. 5b). The decrease in vesicle MD was even more pronounced; it decreased from 1.23 ± 0.15 μm in IFN-γ-activated astrocytes to 0.75 ± 0.08 μm (39.2%, $P \leq 0.05$) and 0.80 ± 0.09 μm (35.0%, $P \leq 0.05$) with the addition of FTY720 or FTY720-P, respectively (Fig. 5c). The DI decreased from 0.36 ± 0.03 in IFN-γ-activated cells to 0.26 ± 0.02 (28.8%, $P \leq 0.05$) and 0.27 ± 0.02 (23.7%, $P \leq 0.05$) with the addition of FTY720 or FTY720-P, respectively (Fig. 5d).

FTY720 and FYT720-P Hinder Secretion of Dextran-Labeled Vesicles from IFN-γ-Activated Astrocytes

In time-lapse confocal images we assessed the extent of ATP-evoked release-productive vesicle fusion events in IFN-γ-activated astrocytes co-treated or not with FTY720 or FYT720-P. The release of cargo from individual vesicles was observed as a rapid decrease of vesicle fluorescence (~ 0.5 s) in successive confocal images, indicating rapid discharge of the fluorescent dextran from the vesicle lumen (Fig. 6 a, b). To assess the extent of secretion events upon 100 μM ATP stimulation, we determined the number of dextran-loaded vesicles at different time points upon cell stimulation and expressed it relative to the initial number estimated at time 0. At 1 and 2 min upon ATP stimulation, the decrease in vesicle number was marginal and similar in cells subjected to different treatments. After 3 min upon ATP stimulation, the decrease in vesicle number was substantial in IFN-γ-activated cells but not in cells co-treated with FTY720 or FYT720-P (Fig. 6c). At 1 min after stimulation, the relative decrease in vesicle number was 3.16 ± 0.69, 3.93 ± 1.43, and 2.68 ± 0.53% for cells treated with IFN-γ, IFN-γ + FTY720, and IFN-γ + FTY720-P, and at 2 min after stimulation, the decrease was 4.92 ± 0.82, 3.41 ± 0.89, and 5.34 ± 1.42%, respectively. At 3 min after stimulation, the vesicle decrease in IFN-γ-activated cells was 14.77 ± 2.86%; the addition of

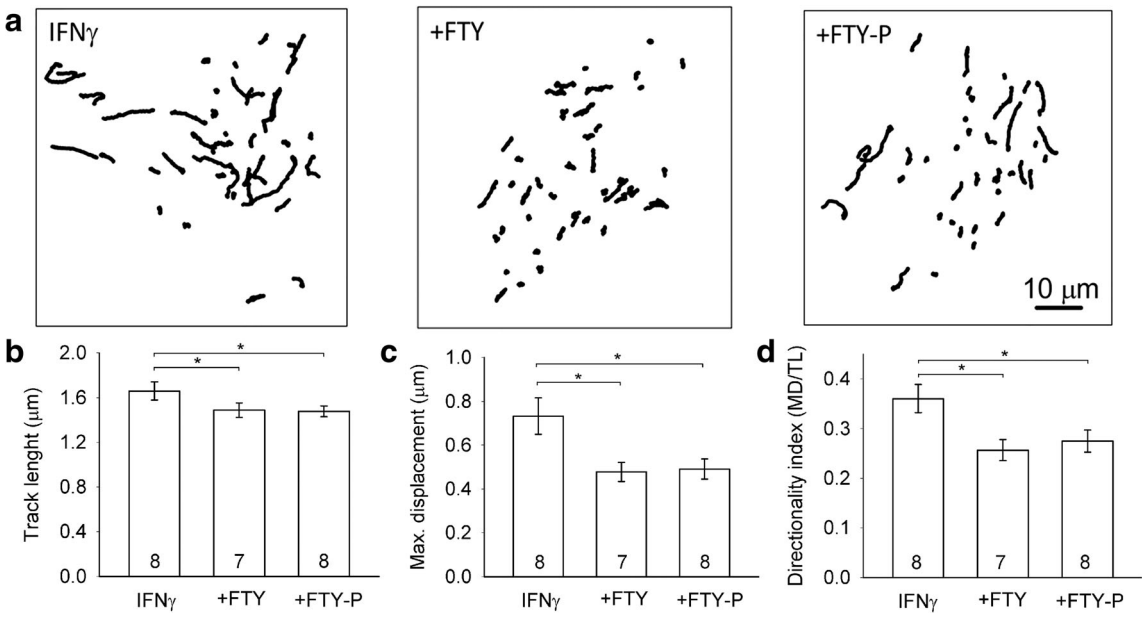

Fig. 5 The mobility of dextran-labeled vesicles is attenuated in IFN-γ-activated astrocytes co-treated with FTY720 or FTY720-P. **a** Reconstructed tracks of dextran-labeled vesicles ($N = 50$) within 1 min in astrocytes activated with IFN-γ (IFN-γ), co-treated with 0.1 μM FTY720 (+FTY) or 0.1 μM FTY720-P (+FTY-P). In IFN-γ-activated cells, the vesicle paths were elongated, whereas in the activated cells co-treated with FTY720 or FTY720-P, the paths were relatively shorter and contorted. Scale bar, 10 μm. **b** Track length, **c** maximal displacement, and **d** directionality index (max. displacement/track length) of dextran-labeled vesicles in astrocytes exposed to different treatments. The addition of FTY720 or FTY720-P significantly attenuated all parameters of vesicle mobility, indicating reduced vesicle speed and directionality. The numbers at the base of the bars indicate the number of cells analyzed for each treatment. *$P \leq 0.05$ versus IFN-γ-activated cells

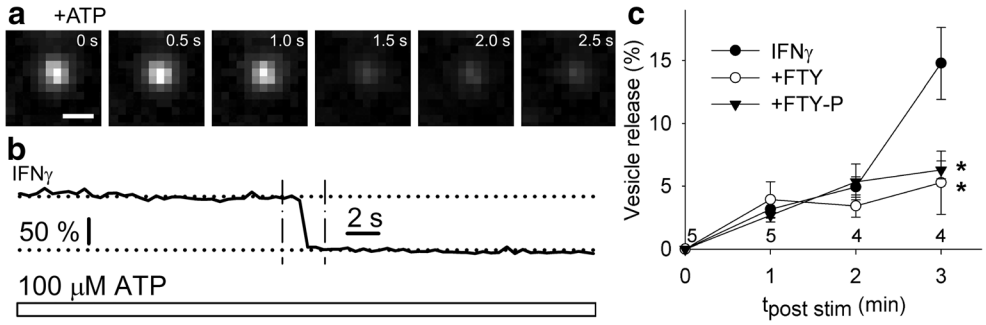

Fig. 6 ATP-evoked secretion of fluorescent dextran from astrocytic vesicles is suppressed in IFN-γ-activated astrocytes co-treated with FTY720 and FTY720-P. **a** Successive confocal images display discharge of fluorescent dextran from an individual vesicle in an IFN-γ-activated astrocyte stimulated by 100 μM ATP (+ATP). The rapid decrease in vesicle fluorescence (~ 0.5 s) indicates rapid discharge of dextran from the vesicle lumen. Scale bar, 0.5 μm. **b** Normalized time-dependent fluorescence decrease recorded in the vesicle displayed in **a**. The horizontal dotted lines indicate the minimum and maximum vesicle fluorescence. The vertical dashed lines indicate the period immediately before and after discharge of dextran (displayed in **a**). The horizontal box indicates the addition of ATP. **c** Discharge of vesicle cargo expressed as a relative decrease in the vesicle number estimated 1, 2, and 3 min after ATP stimulation with respect to time 0 in astrocytes activated with IFN-γ (IFNγ, filled circles), co-treated with FTY720 (+FTY, empty circles), or FTY720-P (+FTY-P, filled triangles). The addition of FTY720 or FTY720-P to IFN-γ-activated astrocytes significantly reduced cargo discharge 3 min after ATP stimulation. *$P \leq 0.05$ versus IFN-γ-activated cells

FTY720 or FTY720-P to activated cells significantly reduced the decrease in vesicle number to 5.27 ± 2.52% ($P \leq 0.05$ vs. IFN-γ-activated cells) and 6.30 ± 0.70% ($P \leq 0.05$ vs. IFN-γ-activated cells), respectively. The decrease in vesicle number reflects the fraction of vesicles that fused with the plasma membrane and released their cargo, although fluorescence bleaching and defocusing may also contribute to the decrease in vesicle fluorescence [75] and give rise to erroneous estimation of the decrease in vesicle number. By assuming that cells exposed to different treatments are similarly affected by bleaching and/or defocusing, the relative values in vesicle decrease can be compared among the different treatments. Therefore, the differences in decrease of vesicle number can be predominantly attributed to the differences in vesicle fusion efficacy primarily affected by cell stimulation and treatment regimes. To independently confirm this finding, we visually counted ATP-evoked discharge events in dextran-labeled vesicles revealed by a sudden decrease in the vesicle fluorescence indicating rapid release of cargo [75]. During the post-stimulation time, the vesicle number decreased by 7.2 ± 4.9, 1.4 ± 0.87, and 3.4 ± 1.89 in cells treated with IFN-γ, IFN-γ + FTY720, and IFN-γ + FTY720-P, respectively (data not shown). The reduction in vesicle number essentially followed the same trend as obtained by automated vesicle detection; however, the decrease in vesicle number was not statistically significant due to relatively high variation between the individual cells.

Discussion

In this study, we provide evidence for direct anti-inflammatory effects of fingolimod (FTY720) and its phosphorylated metabolite (FTY720-P) on cultured astrocytes in the context of brain inflammatory conditions in MS, whereby increased IFN-γ levels may induce astrocytes to adopt a role of facultative APCs. Our findings are consistent with several other reports showing anti-inflammatory and neuroprotective effects of FTY720 [7, 15, 68, 73, 86, 87, 96, 101], most likely as a result of the drug's CNS-intrinsic effects on astrocytes, microglia, and proinflammatory monocytes [68].

The most important observation is that FTY720 or FTY720-P treatment substantially reduced MHC class II expression and increased ADR-β_2 expression in IFN-γ-activated astrocytes. The results revealed that FTY720 attenuated IFN-γ-induced MHC class II expression in a dose-dependent manner, with 23, 54, to 60% decrease in concentrations ranging from 0.01, 0.1, to 0.5 μM FTY720. Similarly, 0.1 μM FTY720-P caused 40% decrease in MHC class II expression. This decrease could significantly contribute to downregulation of the immune response relying on astrocytes acting as brain facultative APCs. It has been shown that in MS, autoreactive T cells must be reactivated in the brain by CNS-resident APCs, which present myelin antigens on their surfaces via the MHC class II complexes, and this triggers the recruitment of innate immune cells, which have important roles in mediating demyelination and axonal damage [32]. Although there is still controversy concerning which cell type, in particular microglia or astrocytes, is the predominant APC in the CNS, it is likely that both cell types participate in a coordinated interplay of immune mechanisms that involve transitions from proinflammatory to immunoregulatory phases of MS [29]. Many indications point to astrocytes as important players in MS in the early activation phase of the disease process [23, 29]. Moreover, astrocytes, in contrast to microglia, are subject to immunosuppressive autonomic regulatory influences that are lost in MS but not in other CNS disorders [23]. Microglia are involved in an injury response in a number of CNS disorders, thus they likely play an effector role in producing CNS tissue damage during the final

pathologic cascade of various diseases [29]. Astrocytes, however, are affected specifically in MS by the loss of a critical regulatory element, the ADR-β_2 receptors [22, 98] that mediate the effects of norepinephrine, which inhibits astrocytic MHC class II expression in normal physiologic conditions [22, 30, 98]. The loss of these receptors facilitates the deviation of astrocytes to function as facultative immunocompetent APCs in the CNS. This specific MS-related astrocyte dysfunction may underlie their critical role in the early activation phase of MS [29].

The fact that reduced MHC class II expression in astrocytes might contribute to the beneficial therapeutic effects in the treatment of MS has been demonstrated by the use of statins. Simvastatin has been shown to reduce MHC class II expression in IFN-γ-activated astrocytes [97], and moreover, a high dose of simvastatin significantly reduced the rate of whole-brain atrophy in patients with secondary progressive MS in a phase II clinical trial [14] and demonstrated a positive effect of the treatment on frontal lobe function and a physical quality-of-life measure [13]. The reduction of MHC class II expression in astrocytes has also been reported for IFN-β [71], which is a widely used initial therapeutic in relapsing–remitting MS [52].

Next, we showed that the addition of FTY720 or FTY720-P to IFN-γ-activated astrocytes increased the expression of ADR-β_2 receptors. IFN-γ treatment caused 1.7-fold increase, whereas the addition of FTY720 or FTY720-P potentiated the increase in ADR-β_2 expression by 3.5-fold. This substantial increase in ADR-β_2 expression could constitute one aspect of the therapeutic efficacy of FTY720, because astrocytes exhibit a reduction of ADR-β_2 in MS, and their increased expression could partially restore ADR-β_2-mediated signaling. Activation of ADR-β_2 results in increased cyclic adenosine monophosphate (cAMP) concentration, which activates protein kinase A (PKA) in astrocytes [40, 90]. Although the cellular mechanism is unknown, in normal conditions, cAMP in astrocytes biochemically prevents the activation of MHC class II molecules by downregulating the class II transactivator protein and suppressing NF-κB-dependent transcriptional activity [21]. In line with our findings, chronic administration of FTY720 increased cAMP levels and promoted cAMP response element binding protein phosphorylation in the hippocampus of Huntington disease transgenic mice R6/1 [58]. Several ADR-β_2 agonists, such as terbutaline, salbutamol, and albuterol, have been reported to exert beneficial effects in animals with experimental autoimmune encephalomyelitis (EAE) [95] or patients with MS [43, 53]. Astrocytic ADR-β_2 dysregulation may contribute to the pathogenesis and progression of MS through deficient inhibition of nitric oxide (NO), proinflammatory cytokine production, and glutamate uptake [24], as well as through deficient glucose transport and glycogenolysis [25], which consequently decrease the energy supply to axons, and finally contributes to progressive axonal degeneration and MS development.

We were interested whether the increase at the protein level reflected increased gene transcription. It turned out that the expression levels of ADR-β_2 mRNA did not parallel alterations in protein abundance. Although activation with IFN-γ and co-treatment with FTY720 or FTY720-P increased the abundance of ADR-β_2 protein, these treatments suppressed ADR-β_2 mRNA levels. One possible explanation for these observations is that IFN-γ, FTY720, and FTY720-P do not increase ADR-β_2 abundance by regulating the expression of the *Adrb2* gene, which suggests a role for post-transcriptional and/or post-translational regulatory mechanisms. Another possibility is that the observed decrease in mRNA levels is a negative feedback response to increased ADR-β_2 abundance and adrenergic signaling via cAMP. For instance, in rat C6 glioma cells [41] as well as other types of cells [4, 34, 81], increased levels of cAMP suppressed ADR-β_2 transcription. Because we measured mRNA levels only at 48 h, downregulation of ADR-β_2 mRNA might therefore be a secondary event that is preceded by an initial increase in its expression.

The next target that we focused on was the NF-κB signaling, which is critically involved in the regulation of immune and inflammatory responses [55]. In MS, NF-κB pathways are changed, leading to increased levels of NF-κB activation in cells, and current MS treatments are found to be directly or indirectly linked to NF-κB pathways and act to adjust the innate and adaptive immune system in patients [49]. The NF-κB transcription factor complex is normally held in the cytoplasm in an inactive form by binding to its inhibitor IκB. Upon activation, IκB is targeted for ubiquitination, allowing phosphorylation of the NF-κB complex and facilitating its translocation to the nucleus, where it can bind to promoter sites to regulate transcription of target genes [39]. It has been previously established that fluorescent microscopy is an appropriate method to observe nuclear translocation of NF-κB subunit Rel A (p65) [61]; therefore, we used a similar method to evaluate the nuclear localization of the NF-κB p65 subunit in treated astrocytes and also quantified the total NF-κB p65 expression. We showed that the addition of FTY720 or FTY720-P to IFN-γ-activated astrocytes significantly decreased the expression of NF-κB p65 with respect to the IFN-γ-activated cells. The decrease was even more pronounced in astrocytes treated only with FTY720 or FTY720-P. The relative nuclear localization of NF-κB p65 was not significantly altered in INF-γ-activated cells; however, the cell treatment with FTY720 or FTY720-P alone significantly reduced the nuclear signal. Nuclear translocation is a relatively fast process and can be observed immediately (30–60 min) upon stimulation by proinflammatory cytokines or bacterial toxins (lipopolysaccharides, LPS) [61]; therefore, the long-term effects of the compounds on p65 nuclear translocation might be less evident. It has been reported that fingolimod inhibited NF-κB nuclear translocation and NO production in astrocytes exposed to inflammatory cytokines

(IL-1, IL-17) or S1P [19]. Similarly, FTY720 treatment led to a significant suppression of NF-κB p65 nuclear translocation in LPS-activated astrocytes, concomitant with decreased production of the pro-inflammatory and neurotoxic mediators IL-6, *tumor necrosis factor* (TNF)-α, GM-CSF, CCL2, and NO [68]. Blocking experiments identified CCL2 and IL-6 as the active components in astrocyte-conditioned medium driving monocyte migration in vitro, whereas TNF-α, GM-CSF, and IL-6 mediated astrocyte neurotoxic activity [68]. Inhibition of NF-κB signaling in astrocytes significantly reduced disease severity and improved functional recovery following EAE by suppressing chronic CNS inflammation and activation of neuro-protective mechanisms [6]. NF-κB inhibition prevented the expression of proinflammatory cytokines, chemokines, and the adhesion molecule VCAM-1 in astrocytes and ameliorated EAE [88].

We then assessed the effects of FTY720 and FTY720-P on the mobility of dextran-loaded vesicles that are enriched with MHC class II molecules in IFN-γ-activated astrocytes [89]. It has already been reported that IFN-γ treatment stimulates vesicle mobility in astrocytes [89]. Moreover, short-term treatment with FTY720 attenuates vesicle mobility in cultured astrocytes [84], and this correlates with increased intracellular Ca^{2+} concentration [77]. Here, we specifically examined whether long-term treatment at nanomolar concentrations induces a similar phenomenon in IFN-γ-activated astrocytes and thus counterbalances the IFN-γ-stimulated increase in vesicle mobility. The addition of FTY720 and FTY720-P to IFN-γ-activated astrocytes decreased vesicle TL, MD, and DI, revealing a decrease in vesicle velocity, as well as directionality of vesicle motion. Vesicle mobility is thus strictly regulated and may affect the immunogenicity of astrocytes in several pathologic conditions [66, 76, 89]. The fact that attenuated mobility of the endocytotic vesicles correlates with decreased MHC class II compartment expression may suggest that vesicle mobility indirectly plays a role in the antigen processing pathway from antigen endocytosis to effective delivery of MHC class II compartments to the plasma membrane. Our findings thus indicate that the cell treatment with FTY720 or FTY720-P decreases the expression of MHC class II molecules and also attenuates the mobility of MHC class II-enriched vesicles that may further reduce surface localization of MHC class II molecules in IFN-γ-activated astrocytes.

The pathway by which MHC class II molecules reach the surface of APCs has been extensively studied; however, it is still not completely understood and may differ among different cell types [54]. It is known that the trafficking of MHC class II compartments in APCs is dependent on the cytoskeletal network [16, 89, 92]. To present at the cell surface, MHC class II-enriched vesicles must reach and fuse with the plasma membrane. Secretory lysosomes could deliver membrane-bound MHC class II molecules to the plasma membrane via exocytosis [9]. Exocytotic release from secretory lysosomes is slow and may begin minutes after astrocyte stimulation with Ca^{2+} ionophores or ATP, which causes immediate increase in intracellular Ca^{2+} concentration [51, 91, 93].

Vesicle fusion in ATP-stimulated IFN-γ-activated astrocytes was observed directly and indirectly by counting dextran-loaded vesicles at different time points after cell stimulation. In IFN-γ-activated cells, the vesicle number firmly decreased 3 min after stimulation, indicating that several vesicles fused to the plasma membrane and released their cargo. This, however, was not the case in FTY720- or FTY720-P-treated IFN-γ-activated cells, where the vesicle number decreased only minutely within the same time after stimulation. This suggests that FTY720 and FTY720-P exerted an inhibitory effect on vesicle fusion, which is in line with our previous work, where we demonstrated that FTY720 inhibited exocytotic secretion of peptide gliotransmitters from ATP-stimulated astrocytes [84]. The observed decrease in fusion activity could be attributed to the attenuated mobility that hinders vesicle delivery to the fusion-competent sites on the plasma membrane and may account for decreased MHC class II expression on the cell surface. The reduced vesicle mobility could thus account for reduced immunogenicity of activated astrocytes in the MS pathology.

Another important aspect of our study is the observation that FTY720 and FTY720-P exerted similar effects on astrocytes in vitro, on their cell count (proliferation), MHC class II, ADR-β_2, NF-κB expression, as well as dextran-labeled vesicle mobility and cargo secretion. FTY720 can be endogenously phosphorylated by sphingosine kinase 2 (Sphk2) [62], which is expressed in astrocytes [15]. In vitro analyses have revealed that ATP-binding cassette transporters [44] and/or S1P transporter spinster homolog 2 (Spns2) [31] mediate S1P release in several types of cells [45, 46, 79], including astrocytes [70], and that FTY720-P can be excreted by the same transport mechanism [38]. Thus, FTY720 may exert effects similar to the exogenously added FTY720-P due to FTY720 phosphorylation by Sphk2 and subsequent release. However, short-term exposure to FTY720 or FTY720-P differentially affects intracellular calcium homeostasis and vesicle mobility [77]. FTY720-P apparently acts immediately via S1P receptors, whereas FTY720 may penetrate through the plasma membrane and act on intracellular targets to exert actions independent of S1P receptors [63, 77].

Conclusions

Our results demonstrated the anti-inflammatory effects of FTY720 and its phosphorylated metabolite (FTY720-P) on cultured astrocytes at therapeutically relevant nanomolar concentrations [57], indicating the potential clinically relevant therapeutic action of fingolimod as an immunomodulatory drug acting directly on astroglia. We observed that FTY720

or FTY720-P treatment substantially reduced MHC class II expression in IFN-γ-activated astrocytes, which may contribute to the downregulation of the immune response involving astrocytes acting as facultative APCs in the brain. Moreover, the treatment increased ADR-β_2 expression, which may further contribute to beneficial effects, because astrocytes in MS plaques lack these receptors. The beneficial effects could be at least partially attributed to the NF-κB signaling cascade, because we further demonstrated that FTY720 or FTY720-P treatment decreased NF-κB B p65 expression (and its nuclear translocation) induced by IFN-γ. Another contributing factor underlying reduced MHC class II expression on astrocytes could be attributed to the attenuated mobility of vesicles that are responsible for the delivery and incorporation of the MHC class II molecules into the plasma membrane. All these effects suggest that fingolimod, an established therapeutic for MS, has direct effects on astroglia, which are important players in the MS pathology. Its anti-inflammatory actions regulate CNS inflammation and thus contribute to its therapeutic efficacy.

Funding The authors acknowledge the financial support from the Slovenian Research Agency (research core funding P3-310 and P3-0043) and projects J3 6790, J3 6789, and J3 7605, CipKeBip, COST Action BM1002, EU COST Action CM1207—GLISTEN, and EU COST Action CM1207—EuroCellNet.

Compliance with Ethical Standards

Conflict of Interest The authors declare that they have no conflict of interest.

Ethical Approval All applicable international, national, and institutional guidelines for the care and use of animals were followed. Care of the experimental animals was in accordance with European and Slovenian legislation (Official Gazette of the RS 38/13; UVHVVR, no. U34401-47/2014/7). This article does not contain any studies with human participants performed by any of the authors.

References

1. Alvarez JI, Katayama T, Prat A (2013) Glial influence on the blood brain barrier. Glia 61(12):1939–1958. https://doi.org/10.1002/glia.22575
2. Araque A, Parpura V, Sanzgiri RP, Haydon PG (1999) Tripartite synapses: glia, the unacknowledged partner. Trends Neurosci 22(5):208–215
3. Billich A, Bornancin F, Dévay P, Mechtcheriakova D, Urtz N, Baumruker T (2003) Phosphorylation of the immunomodulatory drug FTY720 by sphingosine kinases. J Biol Chem 278(48):47408–47415. https://doi.org/10.1074/jbc.M307687200
4. Bouvier M, Collins S, O'Dowd BF, Campbell PT, de Blasi A, Kobilka BK, MacGregor C, Irons GP et al (1989) Two distinct pathways for cAMP-mediated down-regulation of the beta 2-adrenergic receptor. Phosphorylation of the receptor and regulation of its mRNA level. J Biol Chem 264(28):16786–16792
5. Boyle EA, McGeer PL (1990) Cellular immune response in multiple sclerosis plaques. Am J Pathol 137(3):575–584
6. Brambilla R, Persaud T, Hu X, Karmally S, Shestopalov VI, Dvoriantchikova G, Ivanov D, Nathanson L et al (2009) Transgenic inhibition of astroglial NF-kappa B improves functional outcome in experimental autoimmune encephalomyelitis by suppressing chronic central nervous system inflammation. J Immunol 182(5):2628–2640. https://doi.org/10.4049/jimmunol.0802954
7. Brinkmann V (2009) FTY720 (fingolimod) in multiple sclerosis: therapeutic effects in the immune and the central nervous system. Br J Pharmacol 158(5):1173–1182. https://doi.org/10.1111/j.1476-5381.2009.00451.x
8. Brown AM, Baltan Tekkök S, Ransom BR (2004) Energy transfer from astrocytes to axons: the role of CNS glycogen. Neurochem Int 45(4):529–536. https://doi.org/10.1016/j.neuint.2003.11.005
9. Bunbury A, Potolicchio I, Maitra R, Santambrogio L (2009) Functional analysis of monocyte MHC class II compartments. FASEB J 23(1):164–171. https://doi.org/10.1096/fj.08-109439
10. Bustin SA, Benes V, Garson JA, Hellemans J, Huggett J, Kubista M, Mueller R, Nolan T et al (2009) The MIQE guidelines: minimum information for publication of quantitative real-time PCR experiments. Clin Chem 55(4):611–622. https://doi.org/10.1373/clinchem.2008.112797
11. Bö L, Mörk S, Kong PA, Nyland H, Pardo CA, Trapp BD (1994) Detection of MHC class II-antigens on macrophages and microglia, but not on astrocytes and endothelia in active multiple sclerosis lesions. J Neuroimmunol 51(2):135–146
12. Cao Y, Goods BA, Raddassi K, Nepom GT, Kwok WW, Love JC, Hafler DA (2015) Functional inflammatory profiles distinguish myelin-reactive T cells from patients with multiple sclerosis. Sci Transl Med 7(287):287ra274. https://doi.org/10.1126/scitranslmed.aaa8038
13. Chan D, Binks S, Nicholas JM, Frost C, Cardoso MJ, Ourselin S, Wilkie D, Nicholas R et al (2017) Effect of high-dose simvastatin on cognitive, neuropsychiatric, and health-related quality-of-life measures in secondary progressive multiple sclerosis: secondary analyses from the MS-STAT randomised, placebo-controlled trial. Lancet Neurol 16(8):591–600. https://doi.org/10.1016/S1474-4422(17)30113-8
14. Chataway J, Schuerer N, Alsanousi A, Chan D, MacManus D, Hunter K, Anderson V, Bangham CR et al (2014) Effect of high-dose simvastatin on brain atrophy and disability in secondary progressive multiple sclerosis (MS-STAT): a randomised, placebo-controlled, phase 2 trial. Lancet 383(9936):2213–2221. https://doi.org/10.1016/S0140-6736(13)62242-4
15. Choi JW, Gardell SE, Herr DR, Rivera R, Lee CW, Noguchi K, Teo ST, Yung YC et al (2011) FTY720 (fingolimod) efficacy in an animal model of multiple sclerosis requires astrocyte sphingosine 1-phosphate receptor 1 (S1P1) modulation. Proc Natl Acad Sci U S A 108(2):751–756. https://doi.org/10.1073/pnas.1014154108
16. Chow A, Toomre D, Garrett W, Mellman I (2002) Dendritic cell maturation triggers retrograde MHC class II transport from lysosomes to the plasma membrane. Nature 418(6901):988–994. https://doi.org/10.1038/nature01006
17. Chun J, Brinkmann V (2011) A mechanistically novel, first oral therapy for multiple sclerosis: The development of fingolimod (FTY720, Gilenya). Discov Med 12(64):213–228
18. Chun J, Hartung HP (2010) Mechanism of action of oral fingolimod (FTY720) in multiple sclerosis. Clin Neuropharmacol 33(2):91–101. https://doi.org/10.1097/WNF.0b013e3181cbf825
19. Colombo E, Di Dario M, Capitolo E, Chaabane L, Newcombe J, Martino G, Farina C (2014) Fingolimod may support

neuroprotection via blockade of astrocyte nitric oxide. Ann Neurol 76(3):325–337. https://doi.org/10.1002/ana.24217

20. De Keyser J, Laureys G, Demol F, Wilczak N, Mostert J, Clinckers R (2010) Astrocytes as potential targets to suppress inflammatory demyelinating lesions in multiple sclerosis. Neurochem Int 57(4):446–450. https://doi.org/10.1016/j.neuint.2010.02.012
21. De Keyser J, Mostert JP, Koch MW (2008) Dysfunctional astrocytes as key players in the pathogenesis of central nervous system disorders. J Neurol Sci 267(1–2):3–16. https://doi.org/10.1016/j.jns.2007.08.044
22. De Keyser J, Wilczak N, Leta R, Streetland C (1999) Astrocytes in multiple sclerosis lack beta-2 adrenergic receptors. Neurology 53(8):1628–1633
23. De Keyser J, Zeinstra E, Frohman E (2003) Are astrocytes central players in the pathophysiology of multiple sclerosis? Arch Neurol 60(1):132–136
24. De Keyser J, Zeinstra E, Wilczak N (2004) Astrocytic beta2-adrenergic receptors and multiple sclerosis. Neurobiol Dis 15(2):331–339. https://doi.org/10.1016/j.nbd.2003.10.012
25. Dong JH, Chen X, Cui M, Yu X, Pang Q, Sun JP (2012) β2-adrenergic receptor and astrocyte glucose metabolism. J Mol Neurosci 48(2):456–463. https://doi.org/10.1007/s12031-012-9742-4
26. Farina C, Aloisi F, Meinl E (2007) Astrocytes are active players in cerebral innate immunity. Trends Immunol 28(3):138–145. https://doi.org/10.1016/j.it.2007.01.005
27. Foster CA, Howard LM, Schweitzer A, Persohn E, Hiestand PC, Balatoni B, Reuschel R, Beerli C et al (2007) Brain penetration of the oral immunomodulatory drug FTY720 and its phosphorylation in the central nervous system during experimental autoimmune encephalomyelitis: consequences for mode of action in multiple sclerosis. J Pharmacol Exp Ther 323(2):469–475. https://doi.org/10.1124/jpet.107.127183
28. Frohman EM, Frohman TC, Dustin ML, Vayuvegula B, Choi B, Gupta A, van den Noort S, Gupta S (1989) The induction of intercellular adhesion molecule 1 (ICAM-1) expression on human fetal astrocytes by interferon-gamma, tumor necrosis factor alpha, lymphotoxin, and interleukin-1: relevance to intracerebral antigen presentation. J Neuroimmunol 23(2):117–124
29. Frohman EM, Monson NL, Lovett-Racke AE, Racke MK (2001) Autonomic regulation of neuroimmunological responses: implications for multiple sclerosis. J Clin Immunol 21(2):61–73
30. Frohman EM, Vayuvegula B, Gupta S, van den Noort S (1988) Norepinephrine inhibits gamma-interferon-induced major histocompatibility class II (Ia) antigen expression on cultured astrocytes via beta-2-adrenergic signal transduction mechanisms. Proc Natl Acad Sci U S A 85(4):1292–1296
31. Fukuhara S, Simmons S, Kawamura S, Inoue A, Orba Y, Tokudome T, Sunden Y, Arai Y et al (2012) The sphingosine-1-phosphate transporter Spns2 expressed on endothelial cells regulates lymphocyte trafficking in mice. J Clin Invest 122(4):1416–1426. https://doi.org/10.1172/JCI60746
32. Goverman J (2009) Autoimmune T cell responses in the central nervous system. Nat Rev Immunol 9(6):393–407. https://doi.org/10.1038/nri2550
33. Guček A, Vardjan N, Zorec R (2012) Exocytosis in astrocytes: transmitter release and membrane signal regulation. Neurochem Res 37(11):2351–2363. https://doi.org/10.1007/s11064-012-0773-6
34. Hadcock JR, Wang HY, Malbon CC (1989) Agonist-induced destabilization of beta-adrenergic receptor mRNA. Attenuation of glucocorticoid-induced up-regulation of beta-adrenergic receptors. J Biol Chem 264(33):19928–19933
35. Halliday GM, Stevens CH (2011) Glia: initiators and progressors of pathology in Parkinson's disease. Mov Disord 26(1):6–17. https://doi.org/10.1002/mds.23455
36. Harder DR, Zhang C, Gebremedhin D (2002) Astrocytes function in matching blood flow to metabolic activity. News Physiol Sci 17:27–31
37. Hayashi T, Morimoto C, Burks JS, Kerr C, Hauser SL (1988) Dual-label immunocytochemistry of the active multiple sclerosis lesion: major histocompatibility complex and activation antigens. Ann Neurol 24(4):523–531. https://doi.org/10.1002/ana.410240408
38. Hisano Y, Kobayashi N, Kawahara A, Yamaguchi A, Nishi T (2011) The sphingosine 1-phosphate transporter, SPNS2, functions as a transporter of the phosphorylated form of the immunomodulating agent FTY720. J Biol Chem 286(3):1758–1766. https://doi.org/10.1074/jbc.M110.171116
39. Hoffmann A, Baltimore D (2006) Circuitry of nuclear factor kappaB signaling. Immunol Rev 210:171–186. https://doi.org/10.1111/j.0105-2896.2006.00375.x
40. Horvat A, Zorec R, Vardjan N (2016) Adrenergic stimulation of single rat astrocytes results in distinct temporal changes in intracellular Ca(2+) and cAMP-dependent PKA responses. Cell Calcium 59(4):156–163. https://doi.org/10.1016/j.ceca.2016.01.002
41. Hosoda K, Fitzgerald LR, Vaidya VA, Feussner GK, Fishman PH, Duman RS (1995) Regulation of beta 2-adrenergic receptor mRNA and gene transcription in rat C6 glioma cells: effects of agonist, forskolin, and protein synthesis inhibition. Mol Pharmacol 48(2):206–211
42. Kappos L, Radue EW, O'Connor P, Polman C, Hohlfeld R, Calabresi P, Selmaj K, Agoropoulou C et al (2010) A placebo-controlled trial of oral fingolimod in relapsing multiple sclerosis. N Engl J Med 362(5):387–401. https://doi.org/10.1056/NEJMoa0909494
43. Khoury SJ, Healy BC, Kivisäkk P, Viglietta V, Egorova S, Guttmann CR, Wedgwood JF, Hafler DA et al (2010) A randomized controlled double-masked trial of albuterol add-on therapy in patients with multiple sclerosis. Arch Neurol 67(9):1055–1061. https://doi.org/10.1001/archneurol.2010.222
44. Kim RH, Takabe K, Milstien S, Spiegel S (2009) Export and functions of sphingosine-1-phosphate. Biochim Biophys Acta 1791(7):692–696. https://doi.org/10.1016/j.bbalip.2009.02.011
45. Kobayashi N, Nishi T, Hirata T, Kihara A, Sano T, Igarashi Y, Yamaguchi A (2006) Sphingosine 1-phosphate is released from the cytosol of rat platelets in a carrier-mediated manner. J Lipid Res 47(3):614–621. https://doi.org/10.1194/jlr.M500468-JLR200
46. Kobayashi N, Yamaguchi A, Nishi T (2009) Characterization of the ATP-dependent sphingosine 1-phosphate transporter in rat erythrocytes. J Biol Chem 284(32):21192–21200. https://doi.org/10.1074/jbc.M109.006163
47. La Mantia L, Tramacere I, Firwana B, Pacchetti I, Palumbo R, Filippini G (2016) Fingolimod for relapsing-remitting multiple sclerosis. Cochrane Database Syst Rev 4:CD009371. https://doi.org/10.1002/14651858.CD009371.pub2
48. Lee SC, Moore GR, Golenwsky G, Raine CS (1990) Multiple sclerosis: a role for astroglia in active demyelination suggested by class II MHC expression and ultrastructural study. J Neuropathol Exp Neurol 49(2):122–136
49. Leibowitz SM, Yan J (2016) NF-κB pathways in the pathogenesis of multiple sclerosis and the therapeutic implications. Front Mol Neurosci 9:84. https://doi.org/10.3389/fnmol.2016.00084
50. Li C, Zhao R, Gao K, Wei Z, Yin MY, Lau LT, Chui D, Yu AC (2011) Astrocytes: implications for neuroinflammatory pathogenesis of Alzheimer's disease. Curr Alzheimer Res 8(1):67–80
51. Li D, Ropert N, Koulakoff A, Giaume C, Oheim M (2008) Lysosomes are the major vesicular compartment undergoing

Ca2+-regulated exocytosis from cortical astrocytes. J Neurosci 28(30):7648–7658. https://doi.org/10.1523/JNEUROSCI.0744-08.2008

52. Limmroth V, Putzki N, Kachuck NJ (2011) The interferon beta therapies for treatment of relapsing-remitting multiple sclerosis: are they equally efficacious? A comparative review of open-label studies evaluating the efficacy, safety, or dosing of different interferon beta formulations alone or in combination. Ther Adv Neurol Disord 4(5):281–296. https://doi.org/10.1177/1756285611413825
53. Makhlouf K, Weiner HL, Khoury SJ (2002) Potential of beta2-adrenoceptor agonists as add-on therapy for multiple sclerosis: focus on salbutamol (albuterol). CNS Drugs 16(1):1–8
54. Mantegazza AR, Magalhaes JG, Amigorena S, Marks MS (2013) Presentation of phagocytosed antigens by MHC class I and II. Traffic 14(2):135–152. https://doi.org/10.1111/tra.12026
55. Mattson MP, Camandola S (2001) NF-kappaB in neuronal plasticity and neurodegenerative disorders. J Clin Invest 107(3):247–254. https://doi.org/10.1172/JCI11916
56. McFarland HF, Martin R (2007) Multiple sclerosis: a complicated picture of autoimmunity. Nat Immunol 8(9):913–919. https://doi.org/10.1038/ni1507
57. Meno-Tetang GM, Li H, Mis S, Pyszczynski N, Heining P, Lowe P, Jusko WJ (2006) Physiologically based pharmacokinetic modeling of FTY720 (2-amino-2[2-(-4-octylphenyl)ethyl]propane-1,3-diol hydrochloride) in rats after oral and intravenous doses. Drug Metab Dispos 34(9):1480–1487. https://doi.org/10.1124/dmd.105.009001
58. Miguez A, García-Díaz Barriga G, Brito V, Straccia M, Giralt A, Ginés S, Canals JM, Alberch J (2015) Fingolimod (FTY720) enhances hippocampal synaptic plasticity and memory in Huntington's disease by preventing p75NTR up-regulation and astrocyte-mediated inflammation. Hum Mol Genet 24(17):4958–4970. https://doi.org/10.1093/hmg/ddv218
59. Miron VE, Schubart A, Antel JP (2008) Central nervous system-directed effects of FTY720 (fingolimod). J Neurol Sci 274(1–2):13–17. https://doi.org/10.1016/j.jns.2008.06.031
60. Nikcevich KM, Gordon KB, Tan L, Hurst SD, Kroepfl JF, Gardinier M, Barrett TA, Miller SD (1997) IFN-gamma-activated primary murine astrocytes express B7 costimulatory molecules and prime naive antigen-specific T cells. J Immunol 158(2):614–621
61. Noursadeghi M, Tsang J, Haustein T, Miller RF, Chain BM, Katz DR (2008) Quantitative imaging assay for NF-kappaB nuclear translocation in primary human macrophages. J Immunol Methods 329(1–2):194–200. https://doi.org/10.1016/j.jim.2007.10.015
62. Paugh SW, Payne SG, Barbour SE, Milstien S, Spiegel S (2003) The immunosuppressant FTY720 is phosphorylated by sphingosine kinase type 2. FEBS Lett 554(1–2):189–193
63. Payne SG, Oskeritzian CA, Griffiths R, Subramanian P, Barbour SE, Chalfant CE, Milstien S, Spiegel S (2007) The immunosuppressant drug FTY720 inhibits cytosolic phospholipase A2 independently of sphingosine-1-phosphate receptors. Blood 109(3):1077–1085. https://doi.org/10.1182/blood-2006-03-011437
64. Philips T, Robberecht W (2011) Neuroinflammation in amyotrophic lateral sclerosis: role of glial activation in motor neuron disease. Lancet Neurol 10(3):253–263. https://doi.org/10.1016/S1474-4422(11)70015-1
65. Potokar M, Kreft M, Pangrsic T, Zorec R (2005) Vesicle mobility studied in cultured astrocytes. Biochem Biophys Res Commun 329(2):678–683. https://doi.org/10.1016/j.bbrc.2005.02.030
66. Potokar M, Stenovec M, Kreft M, Gabrijel M, Zorec R (2011) Physiopathologic dynamics of vesicle traffic in astrocytes. Histol Histopathol 26(2):277–284
67. Ransohoff RM, Estes ML (1991) Astrocyte expression of major histocompatibility complex gene products in multiple sclerosis brain tissue obtained by stereotactic biopsy. Arch Neurol 48(12):1244–1246
68. Rothhammer V, Kenison JE, Tjon E, Takenaka MC, de Lima KA, Borucki DM, Chao CC, Wilz A et al (2017) Sphingosine 1-phosphate receptor modulation suppresses pathogenic astrocyte activation and chronic progressive CNS inflammation. Proc Natl Acad Sci U S A 114(8):2012–2017. https://doi.org/10.1073/pnas.1615413114
69. Ruijter JM, Ramakers C, Hoogaars WM, Karlen Y, Bakker O, van den Hoff MJ, Moorman AF (2009) Amplification efficiency: linking baseline and bias in the analysis of quantitative PCR data. Nucleic Acids Res 37(6):e45. https://doi.org/10.1093/nar/gkp045
70. Sato K, Malchinkhuu E, Horiuchi Y, Mogi C, Tomura H, Tosaka M, Yoshimoto Y, Kuwabara A et al (2007) Critical role of ABCA1 transporter in sphingosine 1-phosphate release from astrocytes. J Neurochem 103(6):2610–2619. https://doi.org/10.1111/j.1471-4159.2007.04958.x
71. Satoh J, Paty DW, Kim SU (1995) Differential effects of beta and gamma interferons on expression of major histocompatibility complex antigens and intercellular adhesion molecule-1 in cultured fetal human astrocytes. Neurology 45(2):367–373
72. Schwartz JP, Wilson DJ (1992) Preparation and characterization of type 1 astrocytes cultured from adult rat cortex, cerebellum, and striatum. Glia 5(1):75–80. https://doi.org/10.1002/glia.440050111
73. Sehrawat S, Rouse BT (2008) Anti-inflammatory effects of FTY720 against viral-induced immunopathology: role of drug-induced conversion of T cells to become Foxp3+ regulators. J Immunol 180(11):7636–7647
74. Soos JM, Morrow J, Ashley TA, Szente BE, Bikoff EK, Zamvil SS (1998) Astrocytes express elements of the class II endocytic pathway and process central nervous system autoantigen for presentation to encephalitogenic T cells. J Immunol 161(11):5959–5966
75. Stenovec M, Kreft M, Poberaj I, Betz WJ, Zorec R (2004) Slow spontaneous secretion from single large dense-core vesicles monitored in neuroendocrine cells. FASEB J 18(11):1270–1272. https://doi.org/10.1096/fj.03-1397fje
76. Stenovec M, Milosevic M, Petrusic V, Potokar M, Stevic Z, Prebil M, Kreft M, Trkov S et al (2011) Amyotrophic lateral sclerosis immunoglobulins G enhance the mobility of Lysotracker-labelled vesicles in cultured rat astrocytes. Acta Physiol (Oxford) 203(4):457–471. https://doi.org/10.1111/j.1748-1716.2011.02337.x
77. Stenovec M, Trkov S, Kreft M, Zorec R (2014) Alterations of calcium homoeostasis in cultured rat astrocytes evoked by bioactive sphingolipids. Acta Physiol (Oxford) 212(1):49–61. https://doi.org/10.1111/apha.12314
78. Stenovec M, Trkov S, Lasič E, Terzieva S, Kreft M, Rodríguez Arellano JJ, Parpura V, Verkhratsky A et al (2016) Expression of familial Alzheimer disease presenilin 1 gene attenuates vesicle traffic and reduces peptide secretion in cultured astrocytes devoid of pathologic tissue environment. Glia 64(2):317–329. https://doi.org/10.1002/glia.22931
79. Takabe K, Kim RH, Allegood JC, Mitra P, Ramachandran S, Nagahashi M, Harikumar KB, Hait NC et al (2010) Estradiol induces export of sphingosine 1-phosphate from breast cancer cells via ABCC1 and ABCG2. J Biol Chem 285(14):10477–10486. https://doi.org/10.1074/jbc.M109.064162
80. Tan L, Gordon KB, Mueller JP, Matis LA, Miller SD (1998) Presentation of proteolipid protein epitopes and B7-1-dependent activation of encephalitogenic T cells by IFN-gamma-activated SJL/J astrocytes. J Immunol 160(9):4271–4279
81. Tholanikunnel BG, Granneman JG, Malbon CC (1995) The M(r) 35,000 beta-adrenergic receptor mRNA-binding protein binds

transcripts of G-protein-linked receptors which undergo agonist-induced destabilization. J Biol Chem 270(21):12787–12793
82. Tian GF, Azmi H, Takano T, Xu Q, Peng W, Lin J, Oberheim N, Lou N et al (2005) An astrocytic basis of epilepsy. Nat Med 11(9): 973–981. https://doi.org/10.1038/nm1277
83. Traugott U, Scheinberg LC, Raine CS (1985) On the presence of Ia-positive endothelial cells and astrocytes in multiple sclerosis lesions and its relevance to antigen presentation. J Neuroimmunol 8(1):1–14
84. Trkov S, Stenovec M, Kreft M, Potokar M, Parpura V, Davletov B, Zorec R (2012) Fingolimod—a sphingosine-like molecule inhibits vesicle mobility and secretion in astrocytes. Glia 60(9):1406–1416. https://doi.org/10.1002/glia.22361
85. Tuomi JM, Voorbraak F, Jones DL, Ruijter JM (2010) Bias in the Cq value observed with hydrolysis probe based quantitative PCR can be corrected with the estimated PCR efficiency value. Methods 50(4):313–322. https://doi.org/10.1016/j.ymeth.2010.02.003
86. van Doorn R, Nijland PG, Dekker N, Witte ME, Lopes-Pinheiro MA, van het Hof B, Kooij G, Reijerkerk A et al (2012) Fingolimod attenuates ceramide-induced blood-brain barrier dysfunction in multiple sclerosis by targeting reactive astrocytes. Acta Neuropathol 124(3):397–410. https://doi.org/10.1007/s00401-012-1014-4
87. Van Doorn R, Van Horssen J, Verzijl D, Witte M, Ronken E, Van Het Hof B, Lakeman K, Dijkstra CD et al (2010) Sphingosine 1-phosphate receptor 1 and 3 are upregulated in multiple sclerosis lesions. Glia 58(12):1465–1476. https://doi.org/10.1002/glia.21021
88. van Loo G, De Lorenzi R, Schmidt H, Huth M, Mildner A, Schmidt-Supprian M, Lassmann H, Prinz MR et al (2006) Inhibition of transcription factor NF-kappaB in the central nervous system ameliorates autoimmune encephalomyelitis in mice. Nat Immunol 7(9):954–961. https://doi.org/10.1038/ni1372
89. Vardjan N, Gabrijel M, Potokar M, Svajger U, Kreft M, Jeras M, de Pablo Y, Faiz M et al (2012) IFN-γ-induced increase in the mobility of MHC class II compartments in astrocytes depends on intermediate filaments. J Neuroinflammation 9:144. https://doi.org/10.1186/1742-2094-9-144
90. Vardjan N, Kreft M, Zorec R (2014) Dynamics of β-adrenergic/cAMP signaling and morphological changes in cultured astrocytes. Glia 62(4):566–579. https://doi.org/10.1002/glia.22626
91. Vardjan N, Parpura V, Zorec R (2016) Loose excitation-secretion coupling in astrocytes. Glia 64(5):655–667. https://doi.org/10.1002/glia.22920
92. Vascotto F, Lankar D, Faure-André G, Vargas P, Diaz J, Le Roux D, Yuseff MI, Sibarita JB et al (2007) The actin-based motor protein myosin II regulates MHC class II trafficking and BCR-driven antigen presentation. J Cell Biol 176(7):1007–1019. https://doi.org/10.1083/jcb.200611147
93. Verkhratsky A, Matteoli M, Parpura V, Mothet JP, Zorec R (2016) Astrocytes as secretory cells of the central nervous system: idiosyncrasies of vesicular secretion. EMBO J 35(3):239–257. https://doi.org/10.15252/embj.201592705
94. Verkhratsky A, Nedergaard M (2018) Physiology of astroglia. Physiol Rev 98(1):239–389. https://doi.org/10.1152/physrev.00042.2016
95. Wiegmann K, Muthyala S, Kim DH, Arnason BG, Chelmicka-Schorr E (1995) Beta-adrenergic agonists suppress chronic/relapsing experimental allergic encephalomyelitis (CREAE) in Lewis rats. J Neuroimmunol 56(2):201–206
96. Wu C, Leong SY, Moore CS, Cui QL, Gris P, Bernier LP, Johnson TA, Séguéla P et al (2013) Dual effects of daily FTY720 on human astrocytes in vitro: relevance for neuroinflammation. J Neuroinflammation 10:41. https://doi.org/10.1186/1742-2094-10-41
97. Zeinstra E, Wilczak N, Chesik D, Glazenburg L, Kroese FG, De Keyser J (2006) Simvastatin inhibits interferon-gamma-induced MHC class II up-regulation in cultured astrocytes. J Neuroinflammation 3(16):16. https://doi.org/10.1186/1742-2094-3-16
98. Zeinstra E, Wilczak N, De Keyser J (2000) [3H] dihydroalprenolol binding to beta adrenergic receptors in multiple sclerosis brain. Neurosci Lett 289(1):75–77
99. Zeinstra E, Wilczak N, De Keyser J (2003) Reactive astrocytes in chronic active lesions of multiple sclerosis express co-stimulatory molecules B7-1 and B7-2. J Neuroimmunol 135(1–2):166–171
100. Zeinstra E, Wilczak N, Streefland C, De Keyser J (2000) Astrocytes in chronic active multiple sclerosis plaques express MHC class II molecules. Neuroreport 11(1):89–91
101. Zhang Y, Li X, Ciric B, Ma CG, Gran B, Rostami A, Zhang GX (2017) Effect of fingolimod on neural stem cells: a novel mechanism and broadened application for neural repair. Mol Ther 25(2): 401–415. https://doi.org/10.1016/j.ymthe.2016.12.008